

## Perfusion-Based fMRI: Insights From Animal Models

Afonso C. Silva, PhD\*

Modern functional neuroimaging techniques, including functional magnetic resonance imaging (fMRI), positron emission tomography (PET), and optical imaging of intrinsic signals (OIS), rely on a tight coupling between neural activity and cerebral blood flow (CBF) to visualize brain activity using CBF as a surrogate marker. Because CBF is a uniquely defined physiological parameter, fMRI techniques based on CBF contrast have the advantage of being specific to tissue signal change, and the potential to provide more direct and quantitative measures of brain activation than blood oxygenation level-dependent (BOLD)- or cerebral blood volume (CBV)-based techniques. The changes in CBF elicited by increased neural activity are an excellent index of the magnitude of electrical activity. Increases in CBF are more closely localized to the foci of increased electrical activity, and occur more promptly to the stimulus than BOLD- or CBV-based contrast. In addition, CBF-based fMRI is less affected by confounds from venous drainage common to BOLD. Animal studies of brain activation have yielded considerable insights into the advantages of CBF-based fMRI. Based on results provided by animal studies, CBF fMRI may offer a means of better assessing the magnitude, spatial extent, and temporal response of neural activity, and may be more specific to tissue state. These properties are expected to be particularly useful for longitudinal and quantitative fMRI studies.

**Key Words:** functional magnetic resonance imaging; arterial spin labeling; animal models; cerebral blood flow; spatial resolution; temporal resolution

**J. Magn. Reson. Imaging 2005;22:745–750.**

**Published 2005 Wiley-Liss, Inc.<sup>†</sup>**

MEASUREMENT OF CEREBRAL BLOOD FLOW (CBF) is a very important way of assessing brain tissue viability, metabolism, and function. Due to the tight coupling

between neural activity and CBF, functional neuroimaging techniques such as positron emission tomography (PET), optical imaging of intrinsic signals (OIS), and functional magnetic resonance imaging (fMRI) techniques are having a significant impact in defining regions of the brain that are activated in response to specific stimuli (1). As reviewed in the ISMRM Workshop on Quantitative Cerebral Perfusion Imaging using MRI (March 2004), CBF can be measured noninvasively with MRI by using arterial water as a perfusion tracer (refer to papers by Dr. David C. Alsop and Dr. Eric C. Wong in this issue). With the possibility of measuring CBF with MRI techniques came the measurement of CBF changes elicited by changes in neuronal electrical activity. Because CBF is a uniquely defined physiological parameter, CBF-based fMRI has the advantage among the different fMRI techniques of being specific to functional changes that occur in the tissue, a critical feature for quantitative measurements within subjects and across subjects, and for high-resolution functional mapping. Unlike the conventional blood oxygenation level-dependent (BOLD) technique, the CBF change is an excellent index of magnitude of neural activity change. Thus, CBF-based fMRI is the tool of choice for longitudinal functional imaging studies.

The use of animal models has been of fundamental importance to the development of MRI techniques dedicated to the measurement of CBF. Prior to the use of endogenous water as a perfusion tracer, CBF could be measured following the dynamics of exogenously administered MR-detectable tracers, such as deuterium (2,3), fluorine (4,5), or gadolinium chelates (6,7). The advantages of using an endogenous tracer led to the development of arterial spin labeling (ASL) techniques. The first demonstrations of ASL for measuring regional blood flow were in the rodent brain (8,9). Indeed, the rodent model has been the workhorse for the development of theoretical issues, as well as experimental approaches aimed at elucidating quantification of regional blood flow. For example, issues such as the effects of magnetization transfer (10,11), the transit time from the labeling plane to the detection voxels (12,13), the perfusion territory of specific arterial vessels (14), and complex issues related to the exchange of arterial water with tissue water (10,15–18) have all been studied in the rodent brain. More recently, animal models of functional activation of the brain have been employed with

Cerebral Microcirculation Unit, Laboratory of Functional and Molecular Imaging, National Institute of Neurological Disorders and Stroke, Bethesda, Maryland, USA.

Contract grant sponsor: Intramural Research Program of the NIH, National Institute for Neurological Disorders and Stroke.

\*Address reprint requests to: A.C.S., Cerebral Microcirculation Unit, Laboratory of Functional and Molecular Imaging, National Institute of Neurological Disorders and Stroke, National Institutes of Health, 10 Center Dr., MSC 1065, Building 10, Room B1D106, Bethesda, MD 20892-1065. E-mail: silvaa@ninds.nih.gov

Received February 22, 2005; Accepted September 19, 2005.

DOI 10.1002/jmri.20461

Published online 2 November 2005 in Wiley InterScience (www.interscience.wiley.com).

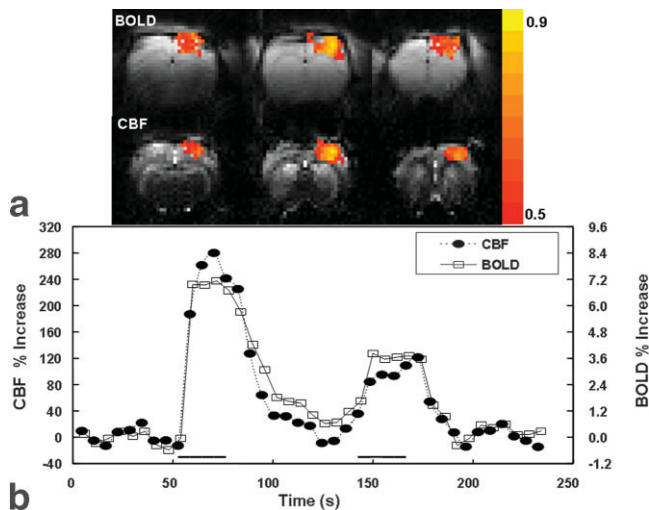


**Figure 1.** High temporal and spatial correlation between BOLD and CBF-based fMRI. **a:** GE-BOLD (top row) and CBF (bottom row) activation maps of the rat brain at 9.4 T upon electrical stimulation of the right forepaw. **b:** Time-course of a nine-pixel ROI placed on the center of the active areas (middle slice in **a**) of the BOLD and CBF maps. The temporal correlation coefficient between the BOLD and the CBF time-courses was 0.92. (Adapted from Silva AC, Lee SP, Yang G, Iadecola C, Kim SG. Simultaneous blood oxygenation level-dependent and cerebral blood flow functional magnetic resonance imaging during forepaw stimulation in the rat. *J Cereb Blood Flow Metab* 1999;19:871–879, with permission of Lippincott Williams & Wilkins.)

great success (19–28) to demonstrate the spatial localization of ASL, the magnitude of signal changes as a function of stimulation parameters, and the temporal aspects of the CBF functional time-course. While similar issues have been studied in humans, the use of animal models in CBF-based fMRI has the advantage of utilizing high-field magnets and state-of-the-art scanners with specialized hardware. With the continued improvement of MRI hardware, both the spatial and the temporal resolutions of fMRI have improved. The higher spatial resolution means better spatial localization of fMRI signal changes. Better temporal resolution also means better spatial localization, as early hemodynamic events are likely to occur close to the site of increased neuronal activity. This paper is aimed at describing the most prominent insights in CBF-based fMRI techniques that have been obtained by the use of animal models.

### SPATIAL SPECIFICITY OF CBF SIGNAL CHANGES

Because of the widespread use of BOLD to map brain function, it is important to compare this type of contrast to well-established physiological functional markers, such as CBF. Animal studies comparing BOLD and CBF regions of activation using fMRI have been recently reported in the rat somatosensory cortex (20–22,29) and in the cat visual cortex (23). These animal studies

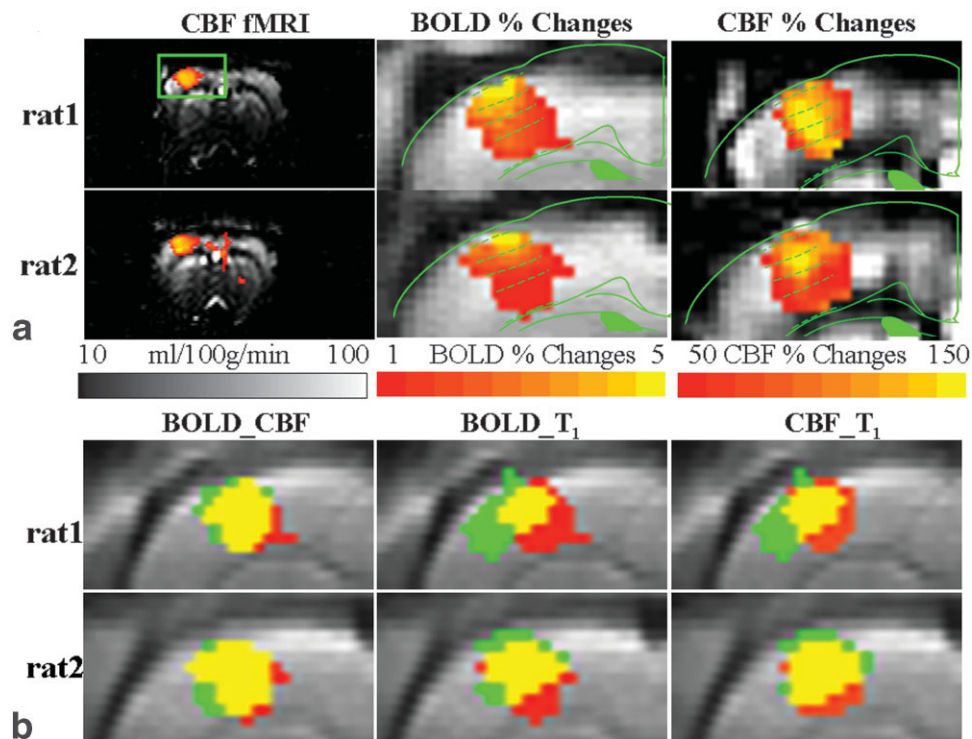


**Figure 2.** Spatial localization of fMRI responses with respect to cortical layers and underlying neuronal activity. **a:** CBF cross-correlation activation maps obtained in the rat at 9.4 T and overlaid on CBF image (left); close-up view of BOLD percent changes shows the highest signal changes in the superficial cortical laminae (middle); and close-up view of CBF percent changes shows the highest signal changes in the middle cortical laminae (right). **b:** Spatial overlap of GE-BOLD and CBF vs. calcium-dependent activity. Left: BOLD (red), CBF (green), and overlap (yellow). Middle: BOLD (red), T1 (green), and overlap (yellow). Right: CBF (red), T1 (green), and overlap (yellow). (Adapted from Duong TQ, Silva AC, Lee SP, Kim SG. Functional MRI of calcium-dependent synaptic activity: Cross correlation with CBF and BOLD measurements. *Magn Reson Med* 2000;43:383–392, with permission of Wiley-Liss Inc., Wiley Publishing Inc., a subsidiary of John Wiley & Sons, Inc.)

have established important considerations regarding the spatial localization of BOLD with respect to CBF and to the expected site of increased electrical activity. For example, Fig. 1 shows gradient-echo BOLD (GE-BOLD) and CBF functional maps of the rat primary somatosensory cortex obtained at 9.4 T during forepaw stimulation. It was determined that the mean separation between the center of the BOLD and the CBF active regions was less than one pixel ( $\sim 500 \mu\text{m}$ ) (29). Thus, good agreement in the spatial location of activation regions was observed. The number of pixels in the BOLD region was strongly correlated to the number of pixels in the CBF region, indicating that CBF is a major driver of positive BOLD signal changes at high magnetic field strengths.

While the localization of the center of mass of BOLD and CBF regions agreed well, the highest CBF changes during somatosensory stimulation (20,22) were observed in cortical layer IV, and not at the surface of the cortex, whereas GE-BOLD images presented the highest changes at the cortical surface, where the large vessels are located (20,30). This can be observed in Fig. 2a, which shows the spatial localization of BOLD- and CBF-based fMRI responses to somatosensory stimulation with respect to the rat cortical layers. Figure 2b shows a comparison of the overlap of BOLD, CBF, and calcium influx, the latter as probed by  $T_1$ -weighted images sensitive to the calcium analog  $\text{Mn}^{++}$  (20). There was a strong agreement between areas showing the highest CBF change and areas showing the highest calcium influx change, both located in layer IV of the somatosensory cortex, suggesting a close correspondence between CBF and synaptic activity. Indeed, the laminar specificity of the CBF response reproduces results obtained with  $[^{14}\text{C}]$ -deoxyglucose and  $[^{14}\text{C}]$ -iodoantipyrine autoradiographic studies in the barrel cortex (31,32).

Such spatial characteristics of ASL-measured CBF response were further examined in cat primary visual cortex by means of the FAIR technique (23). Figure 3 displays representative CBF maps during 1-minute moving gratings of two orthogonal orientations. The rat and cat data demonstrate that stimulus-evoked CBF response is spatially confined to individual submillimeter cortical columns and laminae. Due to the absence of large draining vessel contribution, perfusion-based fMRI signals are more specific to tissue when compared with conventional BOLD contrast. While CBF maintains its high spatial specificity at all magnetic field strengths, the same cannot be said of the BOLD contrast. The functional CBF maps measured with FAIR in response to single-orientation stimulation of the cat visual cortex at 4.7 T were specific to submillimeter columnar structure, in contrast to GE-BOLD, which could not resolve columnar structures (23). This indicates that perfusion-based fMRI provides higher spatial specificity than BOLD fMRI at medium and low magnetic fields such as 4.7 T.

### MAGNITUDE OF SIGNAL CHANGES

The CBF contrast mostly reflects truly perfusing spins that have permeated the capillary walls and entered the

extravascular space (15). Since relative CBF changes are linearly correlated to metabolic changes (33,34), under normal physiological conditions, CBF can play the role of a gold standard for quantifying neuronal activity, as long as quantification of CBF in itself is reasonably accurate. The quantification of absolute CBF values requires suppression of large vessel artifacts, in particular those originated from large arteries. We have observed a 10% to 20% reduction in measured resting CBF values with the use of small to moderate ( $b = 20\text{--}500 \text{ seconds/mm}^2$ ) diffusion-sensitizing gradients in rats (15,22). However, the use of diffusion-sensitizing gradients has no effect on quantifying relative CBF changes during somatosensory stimulation in the rat (22), suggesting that the arterial vasodilatation is proportional to the CBF changes. This is consistent with previous findings of significant arterial cerebral blood volume (CBV) changes during increased CBF (35). Taken together, the contribution of large vessels to functional CBF changes, as measured by the continuous ASL technique, does not alter tissue-level relative CBF changes.

The relative magnitude of CBF and BOLD signal changes during somatosensory stimulation in rat have been extensively compared at 9.4 T (19–22,29). Figure 4 shows a plot of the percent change in the spin-echo BOLD (SE-BOLD) signal vs. the percent change in CBF. Individual diffusion-sensitized fMRI data obtained from 10 animals were plotted. The relationship between relative BOLD and CBF changes was identical in all groups, indicating that the presence of diffusion-weighting gradients did not affect either the percent BOLD change or the percent CBF change. This result is consistent with previous observations that the SE-BOLD contrast has its origin in extravascular dynamic averaging effects around small vessels (36), and therefore our results show excellent correlation between SE-BOLD and CBF changes during functional stimulation at high spatial resolution. When the large vascular component is suppressed, CBF- and BOLD-based fMRI signals are closely coupled spatially and originate from a similar anatomical location, within a single submillimeter voxel. However, the relationship between BOLD and CBF changes is highly nonlinear (Fig. 4), especially at high CBF changes. This nonlinear relation should be taken into account when trying to use BOLD-based fMRI as a quantitative method for mapping neuronal activity. Such a relationship can also be found in CBF and GE-BOLD signals obtained from a large region of interest (ROI), but not on a pixel-by-pixel basis (37).

### TEMPORAL CHARACTERISTICS

The temporal resolution of ASL methods for quantifying CBF is inherently low. Proper perfusion contrast is achieved only when enough time is allowed for the labeled spins to travel into the ROI and exchange with tissue spins. In addition, it is necessary to acquire two images — usually in an interleaved manner — to determine CBF: one with spin labeling and another as a control. Thus, the typical temporal resolution of ASL methods is about a few seconds. In order to obtain dynamic CBF changes with high temporal and spatial

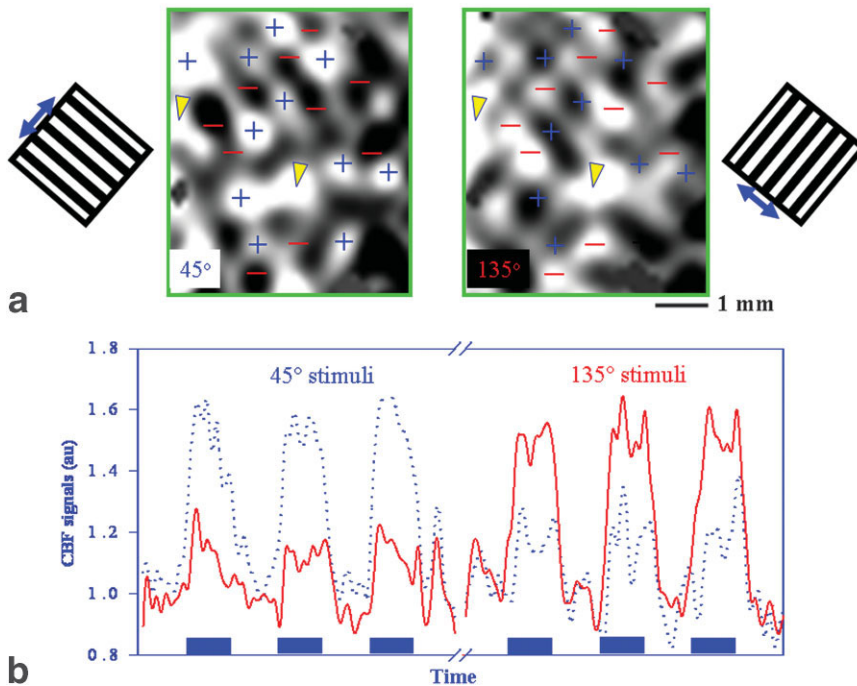


**Figure 3.** Spatial characteristics of CBF-based fMRI response in cat primary visual cortex. **a:** FAIR maps of the CBF response in cat primary visual cortex to two orthogonal moving grating stimuli at 4.7 T. CBF-activated pixels responding to the 45° stimulus were marked with + signs (blue). CBF-activated pixels responding to the 135° stimulus were marked with - signs (red). **b:** The dotted trace (blue) shows the CBF response from pixels activated by the 45° stimulus. The thick trace (red) shows the CBF response from pixels activated by the 135° stimulus. (Adapted from Duong TQ, Kim DS, Ugurbil K, Kim SG. Localized cerebral blood flow response at sub-millimeter columnar resolution. *Proc Natl Acad Sci USA* 2001;98:10904–10909, with permission of the National Academy of Sciences.)

resolution, we have recently devised a novel MRI technique, coined pseudocontinuous ASL (PCASL) (19). The PCASL technique consists of using a short ASL radio frequency (RF) pulse in conjunction with an ultrafast imaging sequence, such as echo planar or spiral imaging. The ASL RF pulse is made short to allow for high

temporal resolution, but long compared to the imaging time so that high labeling duty cycles (and thus efficiency) can be maintained. For example, PCASL has been implemented using 78-msec ASL pulses in conjunction with a 30-msec EPI sequence (19,21). Under these conditions, CBF images could be formed every 108 msec with a labeling efficiency of 59% ( $\alpha = 0.59$ ). In PCASL, two separate experiments are performed: one with spin labeling and the other as a control. Once the CBF images are formed, an analysis of the temporal characteristics of the CBF time-course is desired. For this, a temporal deconvolution of the CBF time-course becomes necessary. This deconvolution is necessary because instantaneous changes in CBF cause slow variations in the MRI signal. The basic principle of the ASL technique is the transfer of the longitudinal magnetization state of the arterial water spins to the tissue spins. This transfer is limited by  $T_{1app}$ ,  $TR$ , and the RF flip angle  $\theta$  and cannot occur instantly. Therefore, step changes in perfusion (and consequently in  $T_{1app}$ ) are only reflected a few seconds later in the tissue magnetization. By performing a deconvolution of the MRI-measured CBF signal with the initial magnetization decay curve, this latency in the MRI-measured CBF response can be removed. After this deconvolution process, the resulting CBF time-course reflects accurately the dynamics of the actual CBF changes.

Figure 5a shows the MRI-estimated CBF time-course (gray) and the deconvolved CBF time-course (black) obtained during somatosensory stimulation in rat using the PCASL technique. The MRI-estimated CBF curve was deconvolved with the initial 10 seconds of the control magnetization decay, generating the deconvolved CBF signal. It can be clearly seen how the CBF response measured with MRI is delayed with respect to the deconvolved curve. It can be noticed from Fig. 5a that the deconvolution adds oscillatory noise to the resulting

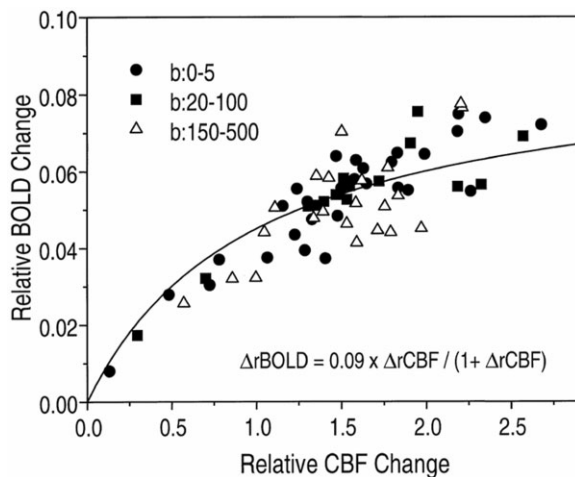


**Figure 4.** Comparison of relative SE-BOLD and CBF signal changes during electrical stimulation of the rat forepaw. The relative changes in BOLD and CBF ( $\Delta rBOLD$  and  $\Delta rCBF$ ) at 9.4 T were respectively calculated as the percent of BOLD or CBF change relative to the resting value. Data were grouped into three diffusion-weighting ranges. There was no difference in the correlation between SE-BOLD and CBF at different diffusion weightings. The solid curve shows the fit of the data to the function indicated on the graph. The b-values are given in seconds/mm<sup>2</sup>. (Adapted from Lee SP, Silva AC, Kim SG. Comparison of diffusion-weighted high-resolution CBF and spin echo BOLD fMRI at 9.4 T. *Magn Reson Med* 2002;47:736–741, with permission of Wiley-Liss Inc., Wiley Publishing Inc., a subsidiary of John Wiley & Sons, Inc.)

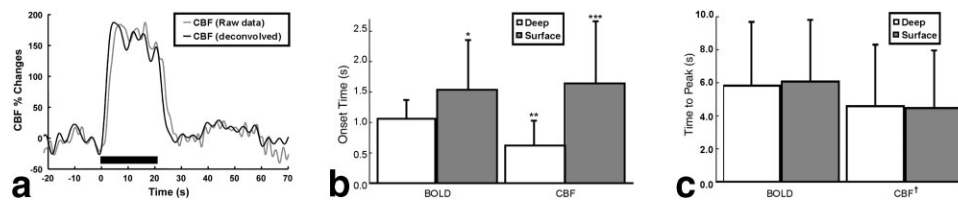


**Figure 5.** Temporal response of CBF and BOLD fMRI signals. **a:** Raw (gray) and deconvolved (black) CBF response curves obtained using pseudocontinuous ASL at 108-msec temporal resolution during electrical stimulation of the rat forepaw. The raw CBF curve was obtained at 9.4 T and was deconvolved with the tissue T1 decay curve to produce the true CBF response. **b:** Averaged onset times of CBF and GE-BOLD at 9.4 T in the surface (gray bars) and deep (white bars) regions of the somatosensory cortex. \*, The onset of the BOLD response in the cortical surface was significantly later than deeper in the cortex ( $P < 0.03$ ). \*\*, CBF changes in the deep cortex occurred earlier than the corresponding BOLD changes ( $P < 0.003$ ). \*\*\*, The onset of superficial CBF changes was significantly delayed compared to deep in cortex ( $P < 0.004$ ). **c:** Averaged time to peak of CBF and BOLD. There were no significant time-to-peak differences across regions within either BOLD ( $P > 0.28$ ) or CBF ( $P > 0.39$ ). †, However, the CBF peak response occurred faster than the BOLD response in both regions ( $P < 0.001$ ). Error bars = 1 SD. (Adapted from Silva AC and Kim SG. Pseudo-continuous arterial spin labeling technique for measuring CBF dynamics with high temporal resolution. *Magn Reson Med* 1999;42:425–429, with permission of Wiley-Liss Inc., Wiley Publishing Inc., a subsidiary of John Wiley & Sons, Inc., and Silva AC, Lee SP, Iadecola C, Kim SG. Early temporal characteristics of cerebral blood flow and deoxyhemoglobin changes during somatosensory stimulation. *J Cereb Blood Flow Metab* 2000;20:201–206, with permission of Lippincott, William & Wilkins.)

curve. However, the CBF changes elicited by this model of activation are very robust, to the point that the results presented here are not compromised by the additional noise introduced by the deconvolution process. Since we used GE-EPI as the readout imaging sequence in our PCASL technique, BOLD signal changes could be measured from the control series of images and directly compared to the corresponding CBF changes. Figure 5b shows the onset time of BOLD and CBF in the superficial and deep regions of the somatosensory cortex following the onset of stimulation. The onset of CBF changes in the deep layers of the somatosensory cortex occurred earlier than the corresponding BOLD changes ( $P < 0.003$ ). However, in the superficial layers, the onset of the CBF response was delayed and it was similar to the latency of the superficial BOLD signal changes. Figure 5c shows the BOLD and CBF times to peak. The CBF peak response occurred faster than the BOLD response in both regions ( $P < 0.001$ ).

### SUMMARY OF PERFUSION-BASED fMRI

Perfusion-based fMRI is specific to the signals caused by functional changes in tissue, a critical feature for proper quantification of the functional response and for high-resolution functional mapping. Unlike the conventional BOLD technique, the CBF change is an excellent index of magnitude of changes in neural activity. Perfusion-based fMRI provides high spatial specificity because contribution of draining veins to CBF-weighted signal is minimal. The perfusion changes induced by neural activity are faster than the BOLD response. By combining ASL with the BOLD technique, both CBF and venous oxygenation level can be obtained, which can be used for examining the sources of the BOLD contrast. Since slow baseline changes can be eliminated by pair-wise subtraction of images, CBF-based functional images can be obtained even when baseline signals modulate due to system instabilities, different gain setting, or physiological changes. Thus, perfusion-based fMRI is the tool of choice for longitudinal func-

tional imaging studies. The use of animal models has been of fundamental importance in providing the above-mentioned insights into this excellent tool for monitoring brain function.

### ACKNOWLEDGMENTS

I acknowledge the organizers of the ISMRM Workshop of Quantitative Cerebral Perfusion Imaging Using MRI: A Technical Perspective, held March 21–23, 2004, in Venice, Italy, for putting together a wonderful and comprehensive program. I also thank Professors Seong-Gi Kim and Timothy Q. Duong for kindly providing some of the figures used in this article.

### REFERENCES

1. Raichle ME. Behind the scenes of functional brain imaging: a historical and physiological perspective. *Proc Natl Acad Sci USA* 1998; 95:765–772.
2. Kim S-G, Ackerman JJH. Quantification of regional blood flow by monitoring of exogenous tracer via nuclear magnetic resonance spectroscopy. *Magn Reson Med* 1990;14:266–282.
3. Detre JA, Subramanian VH, Mitchell MD, Smith DS, Kobayashi A, Zaman A, Leigh Jr JS. Measurement of regional cerebral blood flow in cat brain using intracarotid  $2\text{H}_2\text{O}$  and  $2\text{H}$  NMR imaging. *Magn Reson Med* 1990;14:389–395.
4. Barranco D, Sutton LN, Florin S, Greenberg JH, Sinnwell TM, Ligeti L, McLaughlin AC. Use of  $19\text{F}$  NMR spectroscopy for measurement of cerebral blood flow: a comparative study using microspheres. *J Cereb Blood Flow Metab* 1989;9:886–891.
5. Detre JA, Eskey CJ, Koretsky AP. Measurement of cerebral blood flow in rat brain by  $19\text{F}$ -NMR detection of trifluoromethane wash-out. *Magn Reson Med* 1990;15:4557 [published erratum appears in *Magn Reson Med* 1990;16:179].
6. Villringer A, Rosen BR, Belliveau JW, et al. Dynamic imaging with lanthanide chelates in normal brain: contrast due to magnetic susceptibility effects. *Magn Reson Med* 1988;6:164–174.
7. Rosen BR, Belliveau JW, Buchbinder BR, et al. Contrast agents and cerebral hemodynamics. *Magn Reson Med* 1991;19:285–292.
8. Detre JA, Leigh JS, Williams DS, Koretsky AP. Perfusion imaging. *Magn Reson Med* 1992;23:37–45.
9. Williams DS, Detre JA, Leigh JS, Koretsky AP. Magnetic resonance imaging of perfusion using spin inversion of arterial water. *Proc Natl Acad Sci USA* 1992;89:212–216.

10. Silva AC, Zhang W, Williams DS, Koretsky AP. Estimation of water extraction fractions in rat brain using magnetic resonance measurement of perfusion with arterial spin labeling. *Magn Reson Med* 1997;37:58–68.
11. Zhang W, Silva AC, Williams DS, Koretsky AP. NMR measurement of perfusion using arterial spin labeling without saturation of macromolecular spins. *Magn Reson Med* 1995;33:370–376.
12. Zhang W, Williams DS, Detre JA, Koretsky AP. Measurement of brain perfusion by volume-localized NMR spectroscopy using inversion of arterial water spins: accounting for transit time and cross-relaxation. *Magn Reson Med* 1992;25:362–371.
13. Barbier EL, Silva AC, Kim HJ, Williams DS, Koretsky AP. Perfusion analysis using dynamic arterial spin labeling (DASL). *Magn Reson Med* 1999;41:299–308.
14. Detre JA, Zhang W, Roberts DA, et al. Tissue specific perfusion imaging using arterial spin labeling. *NMR Biomed* 1994;7:75–82.
15. Silva AC, Williams DS, Koretsky AP. Evidence for the exchange of arterial spin-labeled water with tissue water in rat brain from diffusion-sensitized measurements of perfusion. *Magn Reson Med* 1997;38:232–237.
16. Ewing JR, Cao Y, Fenstermacher J. Single-coil arterial spin-tagging for estimating cerebral blood flow as viewed from the capillary: relative contributions of intra- and extravascular signal. *Magn Reson Med* 2001;46:465–475.
17. St Lawrence KS, Frank JA, McLaughlin AC. Effect of restricted water exchange on cerebral blood flow values calculated with arterial spin tagging: a theoretical investigation. *Magn Reson Med* 2000;44:440–449.
18. St Lawrence KS, Lee TY. An adiabatic approximation to the tissue homogeneity model for water exchange in the brain. II. Experimental validation. *J Cereb Blood Flow Metab* 1998;18:1378–1385.
19. Silva AC, Kim SG. Pseudo-continuous arterial spin labeling technique for measuring CBF dynamics with high temporal resolution. *Magn Reson Med* 1999;42:425–429.
20. Duong TQ, Silva AC, Lee SP, Kim SG. Functional MRI of calcium-dependent synaptic activity: cross correlation with CBF and BOLD measurements. *Magn Reson Med* 2000;43:383–392.
21. Silva AC, Lee SP, Iadecola C, Kim SG. Early temporal characteristics of cerebral blood flow and deoxyhemoglobin changes during somatosensory stimulation. *J Cereb Blood Flow Metab* 2000;20:201–206.
22. Lee SP, Silva AC, Kim SG. Comparison of diffusion-weighted high-resolution CBF and spin-echo BOLD fMRI at 9.4 T. *Magn Reson Med* 2002;47:736–741.
23. Duong TQ, Kim DS, Ugurbil K, Kim SG. Localized cerebral blood flow response at submillimeter columnar resolution. *Proc Natl Acad Sci USA* 2001;98:10904–10909.
24. Hyder F, Renken R, Kennan RP, Rothman DL. Quantitative multimodal functional MRI with blood oxygenation level dependent exponential decays adjusted for flow attenuated inversion recovery (BOLD-ED AFFAIR). *Magn Reson Imaging* 2000;18:227–235.
25. Kerskens CM, Hoehn-Berlage M, Schmitz B, Busch E, Bock C, Gyngell ML, Hossmann KA. Ultrafast perfusion-weighted MRI of functional brain activation in rats during forepaw stimulation: comparison with T2-weighted MRI. *NMR Biomed* 1996;9:20–23.
26. Bock C, Schmitz B, Kerskens CM, Gyngell ML, Hossmann KA, Hoehn-Berlage M. Functional MRI of somatosensory activation in rat: effect of hypercapnic up-regulation on perfusion- and BOLD-imaging. *Magn Reson Med* 1998;39:457–461.
27. Franke C, van Dorsten FA, Olah L, Schwandt W, Hoehn M. Arterial spin tagging perfusion imaging of rat brain: dependency on magnetic field strength. *Magn Reson Imaging* 2000;18:1109–1113.
28. Kida I, Maciejewski PK, Hyder F. Dynamic imaging of perfusion and oxygenation by functional magnetic resonance imaging. *J Cereb Blood Flow Metab* 2004;24:1369–1381.
29. Silva AC, Lee SP, Yang G, Iadecola C, Kim SG. Simultaneous blood oxygenation level-dependent and cerebral blood flow functional magnetic resonance imaging during forepaw stimulation in the rat. *J Cereb Blood Flow Metab* 1999;19:871–879.
30. Silva AC, Koretsky AP. Laminar specificity of functional MRI onset times during somatosensory stimulation in rat. *Proc Natl Acad Sci USA* 2002;99:15182–15187.
31. Woolsey TA, Rovainen CM, Cox SB, et al. Neuronal units linked to microvascular modules in cerebral cortex: response elements for imaging the brain. *Cereb Cortex* 1996;6:647–660.
32. Gerrits RJ, Raczynski C, Greene AS, Stein EA. Regional cerebral blood flow responses to variable frequency whisker stimulation: an autoradiographic analysis. *Brain Res* 2000;864:205–212.
33. Sokoloff L, Reivich M, Kennedy C, et al. The [<sup>14</sup>C]deoxyglucose method for the measurement of local cerebral glucose utilization: theory, procedure, and normal values in the conscious and anesthetized albino rat. *J Neurochem* 1977;28:897–916.
34. Fox PT, Raichle ME. Focal physiological uncoupling of cerebral blood flow and oxidative metabolism during somatosensory stimulation in human subjects. *Proc Natl Acad Sci USA* 1986;83:1140–1144.
35. Lee SP, Duong TQ, Yang G, Iadecola C, Kim SG. Relative changes of cerebral arterial and venous blood volumes during increased cerebral blood flow: implications for BOLD fMRI. *Magn Reson Med* 2001;45:791–800.
36. Lee SP, Silva AC, Ugurbil K, Kim SG. Diffusion-weighted spin-echo fMRI at 9.4 T: microvascular/tissue contribution to BOLD signal changes. *Magn Reson Med* 1999;42:919–928.
37. Zhu XH, Kim SG, Andersen P, Ogawa S, Ugurbil K, Chen W. Simultaneous oxygenation and perfusion imaging study of functional activity in primary visual cortex at different visual stimulation frequency: quantitative correlation between BOLD and CBF changes. *Magn Reson Med* 1998;40:703–711.